Journal of Physics: Conference Series

Status of the ATLAS Experiment

To cite this article: Martin Aleksa and the ATLAS Collaboration 2013 *J. Phys.: Conf. Ser.* **452** 012041

Status of the ATLAS Experiment

Martin Aleksa on behalf of the ATLAS Collaboration
CERN, Geneva 23, CH-1211 Geneva, Switzerland
E-mail: martin.aleksa@cern.ch

Abstract.
This document presents an overview of the status of the ATLAS experiment at the CERN Large Hadron Collider at the time of the 5th International Workshop on Top Quark Physics in Winchester (September 2012). The status of the detector and data taking are presented together with some selected physics results and plans for the first long shutdown.

1. The ATLAS Detector

The ATLAS detector [1] is a multipurpose particle physics apparatus with forward-backward symmetric cylindrical geometry at the CERN Large Hadron Collider (LHC). The entire detector (Fig. 1) weighs 7000 tons. It is 44 m long and 25 m in diameter. It is located in an underground cavern at a depth of 100 m, where it surrounds one of the collision points around the 27-km-long LHC ring. The first proton-proton (*pp*) collisions at the LHC were in 2009, and since then the collider has operated at several different center-of-mass energies.

ATLAS is composed of several distinct subdetectors in order to identify and measure the energy and momentum of a variety of particles and so reconstruct the dynamics of the collision. The inner tracking detector (ID) consists of a silicon pixel detector, a silicon microstrip detector, and a straw-tube transition radiation tracker. The ID is surrounded by a thin superconducting solenoid which provides a 2 T magnetic field, and by high granularity liquid-argon (LAr) sampling electromagnetic calorimetry. The electromagnetic calorimeter is divided into a central barrel (pseudorapidity[1] $|\eta| < 1.475$) and end-cap regions on either end of the detector ($1.375 < |\eta| < 2.5$ for the outer wheel and $2.5 < |\eta| < 3.2$ for the inner wheel). In the region matched to the ID ($|\eta| < 2.5$), it is radially segmented into three layers. The first layer has a fine segmentation in η to facilitate e/γ separation from π^0 and to improve the resolution of the shower position and direction measurements. In the region $|\eta| < 1.8$, the electromagnetic calorimeter is preceded by a presampler detector to correct for upstream energy losses. An iron-scintillator/tile calorimeter gives hadronic coverage in the central rapidity range ($|\eta| < 1.7$), while a LAr hadronic end-cap calorimeter provides coverage over $1.5 < |\eta| < 3.2$. The forward regions ($3.2 < |\eta| < 4.9$) are instrumented with LAr calorimeters for both electromagnetic and hadronic measurements. The muon spectrometer surrounds the calorimeters and consists of three large air-core superconducting magnets providing a toroidal field, each with eight coils, a system of precision tracking chambers, and fast detectors for triggering. The combination of all these systems provides charged particle measurements together with efficient and precise lepton and photon measurements in the pseudorapidity range $|\eta| < 2.5$. Jets and missing transverse

[1] The pseudorapidity η is defined in terms of the polar angle θ measured from the beam line as $\eta = -\ln\tan(\theta/2)$.

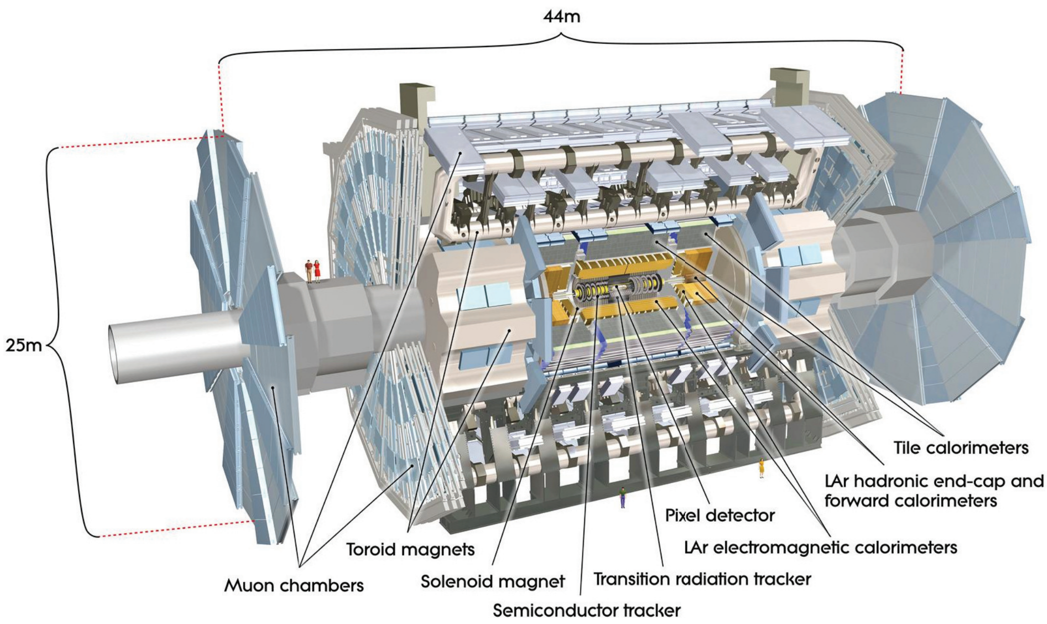

Figure 1. Cutaway drawing of the ATLAS detector showing its main components.

energy $E_{\mathrm{T}}^{\mathrm{miss}}$ are reconstructed using energy deposits over the full coverage of the calorimeters, $|\eta| < 4.9$.

2. Data taking and trigger

Physics data-taking with pp collisions at $\sqrt{s} = 7$ TeV started in March 2011 and ended in October 2011. Between April and December 2012 pp collisions at $\sqrt{s} = 8$ TeV have been recorded. During these periods, LHC delivered to ATLAS an integrated luminosity of 5.6 fb^{-1} at $\sqrt{s} = 7$ TeV and 23.3 fb^{-1} at $\sqrt{s} = 8$ TeV. At the time of the conference in September 2012, only a fraction of the 2012 data-set (14.6 fb^{-1}) was delivered. The exact amount of data used is indicated for each analysis presented here. During both years the data-taking efficiency, signifying the ratio of the recorded and the delivered luminosity, was very high above 93.5 %. After all data quality cuts approximately 90 % of the delivered LHC luminosity was used for physics analysis. A very high fraction of > 96 % of all ATLAS read-out channels was operational during both data-taking periods.

The LHC delivered physics fills with peak instantaneous luminosity of up to $7.7 \times 10^{33}\,\mathrm{cm}^{-2}\mathrm{s}^{-1}$, corresponding to an average of 37 superimposed minimum bias pp collisions per bunch crossing at the start of fills. The ATLAS trigger and offline reconstruction algorithms were extensively optimised during the 2011-12 winter shutdown to make them robust against such high levels of pile-up, beyond the design specifications of the detector. Special care was taken to develop robust algorithms showing flat performance versus pile-up and which minimize CPU usage. The trigger menu was optimised to give a 65 kHz level-1 trigger rate at the start of fill, and a fill-averaged event filter output rate of 400 Hz. Typical trigger thresholds at the event filter are 24-25 GeV transverse momentum for single isolated muons and electrons, 8-18 GeV for di-leptons, 20-35 GeV for diphotons, 20-29 GeV for di-taus and 80 GeV for missing transverse momentum $E_{\mathrm{T}}^{\mathrm{miss}}$.

For example, the main triggers for top physics in the di-lepton and single-lepton (plus jets) channels were single-lepton triggers with slightly increased thresholds and isolation requirements in 2012 compared to 2011. For the all hadronic channel, 5 jet triggers and 1 b-jet + 3 jet triggers were used.

The offline event reconstruction at Tier-0 takes from 15-40 s/event, and was run on up to 7500 CPU cores in parallel to keep up with the data-taking rate. The Worldwide LHC Computing Grid supporting ATLAS continues to be vital, with 150000 simultaneous Monte Carlo simulation and user analysis jobs being run routinely.

3. Some selected physics results

3.1. Standard model cross-sections

A summary of electroweak physics in ATLAS is shown in Fig. 2 where the measured cross-sections of the main electroweak processes are presented together with theoretical predictions [2]. The W and Z vector-boson inclusive cross-sections were measured with $35\,\text{pb}^{-1}$ of integrated luminosity from the 2010 dataset. All other measurements were performed using the 2011 or the 2012 datasets. The top quark pair production cross-section is based on a statistical combination of measurements in the single-lepton, di-lepton and all-hadronic channels. The dark error bar represents the statistical uncertainly. The red error bar represents the full uncertainty, including systematics and luminosity uncertainties. All theoretical expectations were calculated at NLO or higher. The remarkable success of NNLO pQCD calculations together with our present knowledge of the proton parton structure is demonstrated.

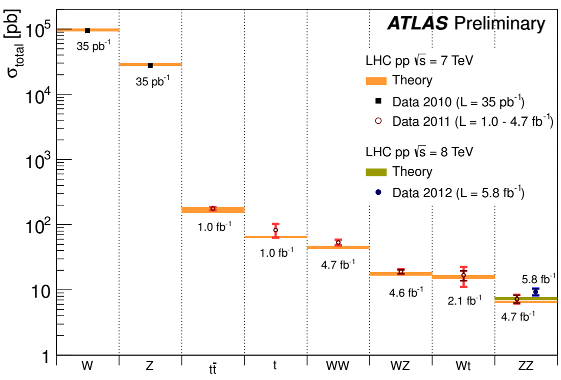

Figure 2. Summary of several standard model total production cross-section measurements compared to the corresponding theoretical expectations [2].

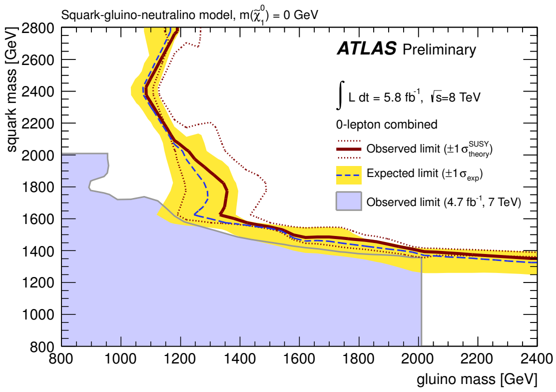

Figure 3. Exclusion limits for the squark and gluino mass in a simplified MSSM scenario with only strong production of gluinos and first- and second-generation squarks, with direct decays to jets and neutralinos [3].

3.2. SUSY searches with 2012 data

Weak scale supersymmetry (SUSY) is an extension of the standard model (SM) that provides a solution to the hierarchy problem by introducing SUSY partners of all SM particles. In the framework of a generic R-parity conserving minimal supersymmetric extension of the SM, SUSY particles are produced in pairs, and the lightest supersymmetric particle is stable and can be a dark matter candidate.

The 2012 dataset has been used to further extend the region of supersymmetric parameter space excluded by previous measurements with the ATLAS detector. First results using the 2012 dataset were presented at the conference. In Fig. 3 a search for squarks and gluinos in

Higgs boson decay	Subsequent decay	Sub-channels	m_H range [GeV]	$\int L dt$ [fb^{-1}]
2011 $\sqrt{s} = 7$ TeV				
$H \to ZZ^{(*)}$	4ℓ	$\{4e, 2e2\mu, 2\mu 2e, 4\mu\}$	110–600	4.8
	$\ell\ell\nu\bar{\nu}$	$\{ee, \mu\mu\} \otimes$ {low, high pile-up}	200–280–600	4.7
	$\ell\ell q\bar{q}$	{b-tagged, untagged}	200–300–600	4.7
$H \to \gamma\gamma$	–	10 categories $\{p_{\mathrm{Tt}} \otimes \eta_\gamma \otimes$ conversion$\} \oplus$ {2-jet}	110–150	4.8
$H \to WW^{(*)}$	$\ell\nu\ell\nu$	$\{ee, e\mu/\mu e, \mu\mu\} \otimes$ {0-jet, 1-jet, 2-jet} $\otimes$ {low, high pile-up}	110–200–300–600	4.7
	$\ell\nu q q'$	$\{e, \mu\} \otimes$ {0-jet, 1-jet, 2-jet}	300–600	4.7
$H \to \tau\tau$	$\tau_{\mathrm{lep}}\tau_{\mathrm{lep}}$	$\{e\mu\} \otimes$ {0-jet} $\oplus \{\ell\ell\} \otimes$ {1-jet, 2-jet, VH}	110–150	4.7
	$\tau_{\mathrm{lep}}\tau_{\mathrm{had}}$	$\{e, \mu\} \otimes$ {0-jet} $\otimes \{E_{\mathrm{T}}^{\mathrm{miss}} < 20$ GeV, $E_{\mathrm{T}}^{\mathrm{miss}} \geqslant 20$ GeV$\}$ $\oplus \{e, \mu\} \otimes$ {1-jet} $\oplus \{\ell\} \otimes$ {2-jet}	110–150	4.7
	$\tau_{\mathrm{had}}\tau_{\mathrm{had}}$	{1-jet}	110–150	4.7
$VH \to Vbb$	$Z \to \nu\nu$	$E_{\mathrm{T}}^{\mathrm{miss}} \in \{120\text{–}160, 160\text{–}200, \geqslant 200$ GeV$\}$	110–130	4.6
	$W \to \ell\nu$	$p_{\mathrm{T}}^{W} \in \{< 50, 50\text{–}100, 100\text{–}200, \geqslant 200$ GeV$\}$	110–130	4.7
	$Z \to \ell\ell$	$p_{\mathrm{T}}^{Z} \in \{< 50, 50\text{–}100, 100\text{–}200, \geqslant 200$ GeV$\}$	110–130	4.7
2012 $\sqrt{s} = 8$ TeV				
$H \to ZZ^{(*)}$	4ℓ	$\{4e, 2e2\mu, 2\mu 2e, 4\mu\}$	110–600	5.8
$H \to \gamma\gamma$	–	10 categories $\{p_{\mathrm{Tt}} \otimes \eta_\gamma \otimes$ conversion$\} \oplus$ {2-jet}	110–150	5.9
$H \to WW^{(*)}$	$e\nu\mu\nu$	$\{e\mu, \mu e\} \otimes$ {0-jet, 1-jet, 2-jet}	110–200	5.8

Table 1. Summary of the individual Higgs decay channels entering the combination [5].

final states containing jets, missing transverse momentum and no high-p_{T} electrons or muons is presented [3]. No excess above the SM expectation is observed. When the neutralino is massless, gluino masses below 1100 GeV are excluded at the 95 % confidence level in a simplified model with only gluinos and the lightest neutralino.

3.3. Standard model Higgs searches

The standard model of particle physics has been tested by many experiments over the last four decades and has been shown to successfully describe high energy particle interactions. However, the mechanism that breaks electroweak symmetry in the SM has not been verified experimentally. This mechanism [4], which gives mass to massive elementary particles, implies the existence of a scalar particle, the SM Higgs boson. The search for the Higgs boson is one of the highlights of the LHC physics programme. The different production and decay modes give rise to a rich experimental phenomenology, with many different analysis channels being used [5] to cover the full mass range of interest, as shown in Tab. 1.

An excess of events is observed near a Higgs mass $m_H = 126\,\mathrm{GeV}$ in the $H \to ZZ^{(*)} \to 4\ell$ and $H \to \gamma\gamma$ channels, both of which provide fully reconstructed candidates with high resolution in invariant mass. These excesses are confirmed by the highly sensitive but low-resolution $H \to WW^{(*)} \to \ell\nu\ell\nu$ channel. The observed local p_0 values from the combination of channels, using the asymptotic approximation, are shown as a function of m_H in Fig. 4 for the low mass range. The significance of the observed excess of events at $m_H = 126\,\mathrm{GeV}$ corresponds to $5.9\,\sigma$. The observed 95 % confidence level exclusion regions are $111 - 122\,\mathrm{GeV}$ and $131 - 559\,\mathrm{GeV}$.

The observed excess corresponds to a best-fit signal strength $\mu = \sigma/\sigma_{\mathrm{SM}} = 1.4 \pm 0.3$ for $m_H = 126\,\mathrm{GeV}$, which is consistent with the SM Higgs boson hypothesis (σ is the observed cross-section and σ_{SM} signifies the expected SM Higgs boson cross-section) . A summary of the individual and combined best-fit values of the strength parameter for a SM Higgs boson mass hypothesis of 126 GeV is shown in Fig. 5. The mass of the observed new particle is estimated using a profile likelihood ratio for the two channels with highest mass resolution. The resulting mass estimate of the observed particle is $126.0 \pm 0.4(\mathrm{stat}) \pm 0.4(\mathrm{sys})\,\mathrm{GeV}$.

4. Plans for the long shutdown 2013 and 2014

The main goal of the long shutdown starting mid February 2013 is to consolidate the LHC magnet inter-connects to be able to operate the LHC at a center-of-mass energy of $\sqrt{s} = 13\,\mathrm{TeV}$

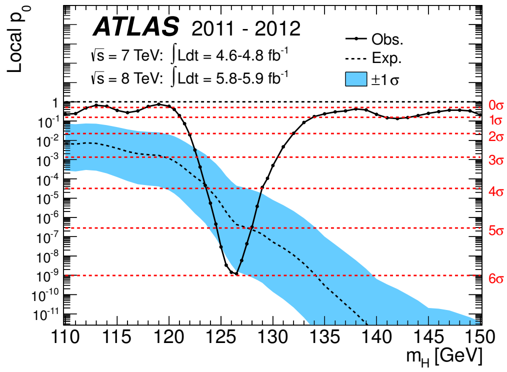

Figure 4. The observed (solid) local p_0 as a function of m_H in the low mass range. The dashed curve shows the expected local p_0 under the hypothesis of a SM Higgs boson signal at that mass with its $\pm 1\sigma$ band [5].

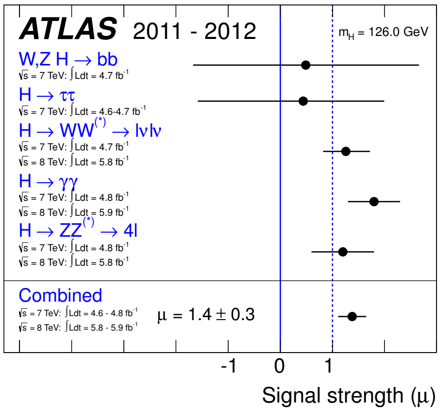

Figure 5. Measurements of the signal strength parameter μ for $m_H = 126\,\text{GeV}$ for the individual channels and their combination [5].

in the years 2015 – 2017. The ATLAS plans during this first long shutdown are the following:

- Adding a new insertable pixel b-layer (IBL) to preserve current physics performance at very high pile-up. Together with the installation of the IBL, a new beam pipe and new pixel services will be installed.
- New evaporative cooling plant for the present inner detector silicon.
- Consolidation of detector elements (e.g. calorimeter power supplies).
- Addition of specific neutron shielding.
- Completion of the installation of endcap extra muon chambers staged in 2003.
- Upgrade of magnet cryogenics.

5. Summary and conclusion

The ATLAS experiment has been performing very well during the LHC *pp* runs in 2011 and 2012. The standard model Higgs boson is excluded at 95 % Confidence Level in the mass range 111 – 559 GeV, except for the narrow region 122 – 131 GeV. In this region, an excess of events with a significance of 5.9 σ is observed. Many interesting physics analyses have been reported and are presented at the ATLAS Collaboration public page [2].

6. Acknowledgements

We thank CERN for the very successful operation of the LHC, as well as the support staff from our institutions without whom ATLAS could not be operated efficiently.

References

[1] ATLAS Collaboration, J. Instrum., 3 S08003 (2008)
[2] ATLAS Collaboration, https://twiki.cern.ch/twiki/pub/AtlasPublic/
[3] ATLAS Collaboration, ATLAS-CONF-2012-109 (2012)
[4] P.W. Higgs, Phys. Lett. 12 (1964) 132; F. Englert, R. Brout, Phys. Rev. Lett. 13 (1964) 321; G.S. Guralnik, C.R. Hagen, T.W.B. Kibble, Phys. Rev. Lett. 13 (1964) 585.
[5] ATLAS Collaboration, Phys. Lett. B716 (2012)